Monitoring Ternary Systems of $C_{12}E_5$/Water/Tetradecane via the Fluorescence of Solvatochromic Probes

Graham Hungerford,* Elisabete M. S. Castanheira, and M. Elisabete C. D. Real Oliveira

Departamento de Física, Universidade do Minho, 4710-057 Braga, Portugal

M. da Graça Miguel and Hugh D. Burrows

Departamento de Química, Universidade de Coimbra, 3004-535 Coimbra, Portugal

Received: August 7, 2001; In Final Form: December 23, 2001

In this work ternary systems of the nonionic surfactant $C_{12}E_5$ ($C_{12}H_{25}(OCH_2CH_2)_5OH$), tetradecane, and water were probed by the use of steady state and time-resolved fluorescence. Microemulsions, which were rich in oil, rich in water, and also both continuous in oil and water, were monitored via the application of solvatochromic fluorescent probes. The hydrophobic laser dye Nile Red was used to report from the side of the oil−surfactant interface, while Prodan, which is soluble in each of the constituent solvents, was used to provide a global picture. To complement these, the hydrophilic dye 4-(2-(dimethylamino)phenyl)-1-methylpyridinium iodide was used to report from the side of the water−surfactant interface. The results show the partitioning of the probes into different environments within the ternary systems as evident from the solvatochromic shift in the emission spectra, uncovering similarities between the water-rich and bicontinuous regions in terms of polarity. Estimates for the polarity of the environments in which the fluorophores are solubilized are made in terms of the $E_{T(30)}$ parameter scale. The time-resolved kinetics of some of the probes have been found to be viscosity dependent, which brought out similarities between the bicontinuous and oil-rich regions along with the observation of the effect of solvent relaxation in these ternary systems.

Introduction

Among the different fluorescence techniques available for studying microemulsions the use of solvatochromic probes is attractive, as a single probe can provide information concerning the range of environments found in these systems. Our interest has been in uncovering information relating to ternary systems involving the nonionic polyoxyethylene surfactant $C_{12}E_5$ ($C_{12}H_{25}(OCH_2CH_2)_5OH$). This is a neutral surfactant consisting of a polyoxyethylene headgroup and an alkyl chain tail. The phase behavior of ternary systems of this surfactant in the presence of an alkane and water have been well studied,[1−9] and these systems have, intriguingly, been found under certain conditions of composition and temperature to form phases that are simultaneously continuous in both water and oil.[10−12] This is of both practical and theoretical importance, and although evidence exists for these phases,[1−3,11] further experimental data are required to fully explain their exact structure. We have previously made use of the excimer-forming properties of pyrene to monitor such systems.[13] Another possible route to elucidate further information is the use of solvatochromic probes. These have found many applications in areas of biology[14] and in the study of micellar systems.[15−17] The interest in their usage stems from the fact that their peak emission wavelength is highly dependent on the dielectric constant of their environment. Hence, in microheterogeneous media a probe molecule partitioned between different environments is capable of reporting on both simultaneously and an initial study has been performed on the so-called bicontinuous region in $C_{12}E_5$ ternary systems.[18]

Two probes of particular note are Prodan[19] and Nile Red.[20] The former has found usage in numerous applications, including as a probe for proteins[21] and micellar media.[15−17] The origin of the solvatochromic properties of Prodan has been a matter of debate with discussion of the presence of a twisted intramolecular charge state. Although it exhibits charge transfer behavior, solvation equilibria have also been used to describe its properties.[22] This probe also has a wide range of solubility, making it suitable to access a wide range of sites within microheterogeneous media. In the ternary system we are interested in studying it was found to be soluble in all three component solvents. The laser dye Nile Red has also proved useful, especially when employed as an extrinsic protein label.[23,24] This probe has a hydrophobic nature (low solubility and fluorescence in water) and therefore has demonstrated value to study biological membranes,[20] with their hydrocarbon-like environments. Its spectroscopic properties in the confinement of micelles[25,26] and γ-cyclodextrin[27] have also been investigated. Both the steady state and time-resolved fluorescence properties of this dye have been found to be highly dependent on its environment.[28,29] As well as its usage in probing microheterogeneous media Nile Red has been employed to measure solvent polarity and compared to Reichardt's pyridinium betaine dye $E_{T(30)}$ scale.[30] Because of these properties, these two probes appear well suited for use with the $C_{12}E_5$ ternary system.

To complement Prodan and Nile Red, we chose the hydrophilic dimethylaminostibazolium dye 4-Di-1-ASP (pyridinium, 4-(2-(dimethylamino)phenyl)-1-methyl, iodide). This dye has also been reported as having polarity- and viscosity-dependent spectroscopic behavior[31] and has been used in work related to dye-induced photoelectric effects in bilayer membranes.[32] Thus,

* Corresponding author. Fax: 00351-253-678981. E-mail: graham@fisica.uminho.pt.

10.1021/jp013047v CCC: $22.00
Published on Web 03/29/2002

this probe should report from the aqueous side of the water−surfactant−alkane boundary and Nile Red from the hydrocarbon side, while Prodan should partition throughout the ternary system. These probes, with their absorption and emission toward the near-infrared part of the spectrum, also have the advantage that Rayleigh scattered excitation light, with its λ^{-4} dependence, is reduced in comparison to when probes, such as pyrene, that require excitation further into the ultraviolet are used. The absorption spectra of the probes fit well with recently developed solid state excitation sources for measurement time-resolved fluorescence with the advantages of instrumentation for use in this wavelength region.[33]

In this paper we employ the solvatochromic probes Prodan, the hydrophobic Nile Red, and the hydrophilic dye 4-Di-1-ASP to monitor the phase behavior in three regions of a $C_{12}E_5$/water/tetradecane system: the water continuous and oil continuous regions, along with a zone that is simultaneously continuous in both oil and water. This was achieved by observing both the steady state and time-resolved fluorescent behavior of the dyes to elucidate their partitioning and hence provide information concerning the polarity of the environments they encounter.

Experimental Section

Materials. Samples of polyoxyethylene 5 lauryl ether ($C_{12}E_5$) from both Sigma and Nikko Company Japan were used. No differences were observed between results with the two samples. The probes Nile Red from Aldrich, Prodan (6-propionyl-2-

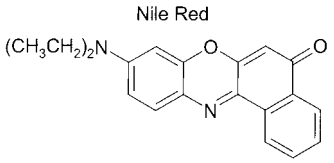

(dimethylamino)naphthalene), and 4-Di-1-ASP (pyridinium,

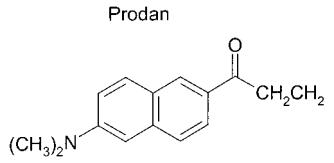

4-(2-(dimethylamino)phenyl)-1-methyl, iodide), both from

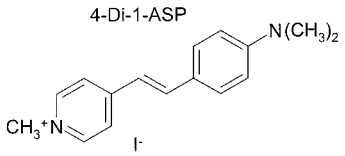

Molecular Probes, were used as received. Solutions were prepared using spectroscopic grade tetradecane and ultrapure water.

Sample Preparation. The samples for the ternary systems involving tetradecane were prepared by combining solutions of 16.6% $C_{12}E_5$ in water with 16.6% $C_{12}E_5$ in tetradecane ($C_{14}H_{30}$) to provide the desired weight fraction ($=C_{14}H_{30}/(H_2O + C_{14}H_{30})$) of tetradecane. The appropriate composition was then added to a cuvette in which the selected amount of probe had been deposited by evaporation from a stock solution in ethanol. The samples were then placed in an ultrasonic bath for mixing and then left for some time to stabilize. The homogeneity of the samples was checked by visual observation at each temperature studied. Three samples were made (for each dye) relating to the different regions of the phase diagram: (i) weight fraction 0.1, an oil-in-water microemulsion (water-rich region), denoted "o/w", existing at 34 °C; (ii) weight fraction 0.45, a region bicontinuous in both oil and water, denoted "bic", existing at 45 °C; (iii) weight fraction 0.9, a water-in-oil microemulsion (oil-rich region), denoted "w/o", present at 57 °C.

Stationary Measurements. The steady state fluorescence and absorption measurements were performed using Spex Fluorolog and Shimadzu UV-3101PC spectrometers, respectively. For the emission and excitation measurements the fluorescence was viewed at right angles and the temperature was maintained using a water jacket on the cuvette holder. For the absorption measurements a Peltier heater was used. Spectral decomposition was performed using Microcal Origin software. In the case of Nile Red the spectrum was fitted to a sum of log-normal component spectra, while for Prodan a sum of Gaussian spectra was used. During the fitting, routine care was taken to ensure no excessively large spectral widths were returned. This meant on occasion limiting the spectral width of the component spectra to 50 nm.

Time-Resolved Fluorescence Measurements. The time-resolved fluorescence measurements were performed using a single-photon counting spectrometer equipped with pulsed nanosecond LED excitation heads (IBH Ltd.) with the equipment running in reverse mode because of the high repetition rate. The detection of the fluorescence, monitored at a right angle to the excitation, was made using a Hamamatsu R2949 side window photomultiplier. The temperature was controlled using a recirculating water heater connected to a jacket on the cuvette holder. The fluorescence decays were measured to 10 000 counts in the peak, unless otherwise indicated, and the instrumental response functions were recorded sequentially using a scattering solution and a nominal time resolution of 100 ps obtained after reconvolution. The decays were analyzed as a sum of exponentials, using a nonlinear least squares reconvolution analysis (IBH Consultants Ltd.), of the form

$$I(t) = \sum_{i=1}^{n} \alpha_i \exp(-t/\tau_i) \qquad (1)$$

The preexponential factors (α_i) are shown normalized to 1 and the errors are taken as three standard deviations. The goodness of fit was judged in terms of both a chi-squared (χ^2) value and weighted residuals.

Results and Discussion

Nile Red. This hydrophobic laser dye was employed to study the ternary system from the hydrocarbon side of the water−surfactant−alkane interface. Both the absorption and fluorescence spectra of this dye are solvatochromic and the position of the peak absorption has been used to provide a solvent polarity scale,[30] while the decay kinetics have also been found to be viscosity dependent.[34] The dye was first studied in the component solvents before observation in the three ternary systems.

Steady State Data. The steady state fluorescence spectra for this dye incorporated into the ternary systems, along with those in pure solvents, are given in Figure 1. This clearly shows the influence of environment on the emission of the dye. In pure tetradecane the spectrum is situated at lower wavelengths and displays some vibrational structure, with peak emissions at 538 and 570 nm. In $C_{12}E_5$ the spectrum becomes structureless and shifted to 620 nm, showing the presence of a more polar environment than tetradecane. Nile Red is a hydrophobic probe

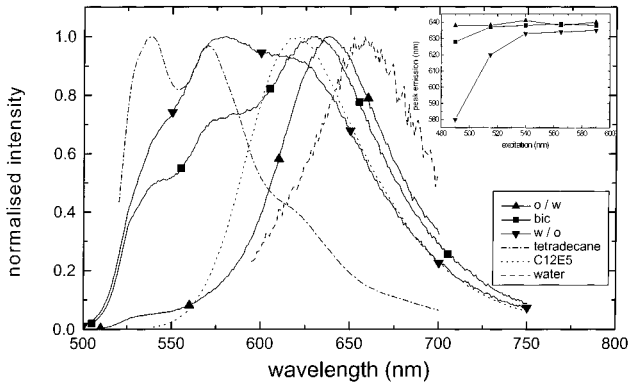

Figure 1. Steady state fluorescence of Nile Red, excited at 490 nm, in the ternary system and in component pure solvents. The effect of changing the excitation wavelength on the peak fluorescence emission is shown in the inset.

and is sparingly soluble in water; however, it is possible to record a weak spectrum peaking close to 660 nm.

In the three-component system, it is clearly visible that Nile Red is distributed among a range of environments. Let us consider each of the regions in turn starting with the water-rich region. In the o/w region it appears that a vast majority of the dye is situated in an environment more polar than pure $C_{12}E_5$, but not as polar as water. This indicates that the Nile Red is situated within the micelle structure close to the headgroup where it experiences the elevated polarity of the surrounding water or the headgroup conformation produces an elevated dielectric constant. As the absorption spectrum of this dye is solvatochromic, by exciting at different wavelengths one would expect to change the peak emission wavelength if a variety of environments were encountered. The Figure 1 inset shows these data for Nile Red in the ternary systems. In the o/w region the peak emission range is small, which indicates that most of the Nile Red is occupying a relatively homogeneous environment. It should be noted however that a small emission could be observed close to 535 nm, which originates from Nile Red well into the micellar interior.

The spectrum obtained for Nile Red in the bicontinuous region (Figure 1) clearly consists of a substantial quantity in tetradecane, as evident from the shoulders on the spectrum at 538 and 570 nm. Also, there is a large amount of emission from the dye in an environment more polar than pure $C_{12}E_5$, but not as polar as that observed in the o/w region. This can relate to dye situated further from the headgroup of $C_{12}E_5$ than in the o/w region, thus not experiencing the polarity of the water to such an extent. In this region Nile Red may be thought of as occupying the oil channels close to the surfactant tail. Further evidence comes from the data in the inset in Figure 1, which, although showing a little more variation than the data for the water-rich region, show that most of the dye is located in similar environments.

In the case of the oil-rich region (w/o) the spectrum shape is again different, although, unsurprisingly because of the hydrophobic nature of Nile Red, most of the emission stems from tetradecane associated dye. There is also emission with a peak intensity at the same wavelength as dye in an environment of pure $C_{12}E_5$. This leads us to conclude that the probe is situated both in the oil and in the tail region of the surfactant, where it does not sense the higher dielectric constant of the water. Evidence for a partitioning between these two environments comes from the wavelength-dependent data (inset, Figure 1). For this region there is a large spread in the emission wavelength, with peak intensity at 580 nm for excitation at 490 nm and an emission just above 630 nm for longer wavelength excitation.

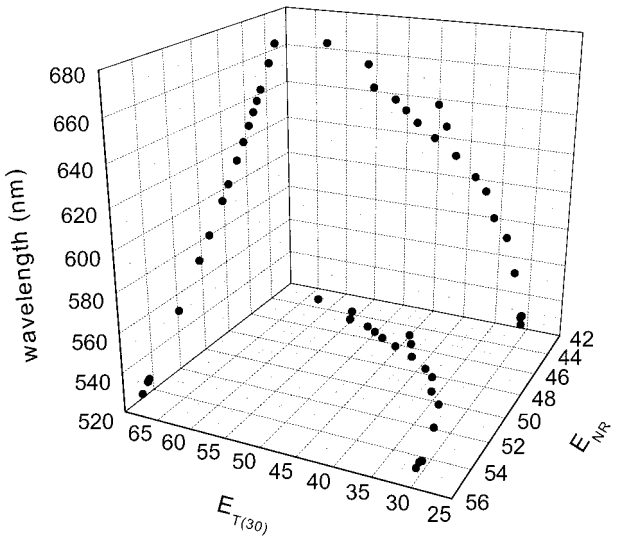

Figure 2. Plot of peak emission wavelength of Nile Red in various solvents in relation to the $E_{T(30)}$ scale and a Nile Red transition energy scale (E_{NR}).

As the absorption spectrum of Nile Red has previously been employed by Deye et al. to measure solvent polarity,[30] we decided to attempt to quantify the polarity of the environments encountered by this probe. This was done by measuring both the absorption and emission spectra in a series of solvents (both protic and nonprotic). As the emphasis of this paper relates to fluorescence emission, an attempt to extend Deye's work by using the Nile Red fluorescence spectrum to measure the solvent polarity was made. Figure 2 shows a plot relating the peak fluorescence of the dye to a Nile Red emission scale, E_{NR} (obtained in a manner similar to that of the absorption scale by conversion of wavelength to transition energies,[30] i.e., $E_{NR} = 28600/(\text{nm})$ kcal mol^{-1}) and the $E_{T(30)}$ scale, for which units of kcal mol^{-1} are used throughout. From analysis of the absorption spectrum, using our solvent selection, we obtained a similar trend comparing the E_{NR} and $E_{T(30)}$ scales to that found by Deye and this is also reflected in the fluorescence data in Figure 2. A comparison between the peak fluorescence of Nile Red and the $E_{T(30)}$ scale does not yield a linear relationship, and this may be attributed to a higher degree of hydrogen bonding encountered using the betaine dye.

Considering the peak emission values obtained for Nile Red incorporated in the ternary systems, this yields E_{NR} values of 44.8, 45.1, and 49.3 for the o/w, bic, and w/o systems, respectively. From the plot in Figure 2 these can be roughly related to respective $E_{T(30)}$ values of 51.4, 49.2, and 35.5. However, these values are approximate as each measured spectrum is the sum of several component spectra, so deconvolution is required to gain a more accurate picture of the partitioning of Nile Red in this system.

Decomposition of Fluorescence Spectra. To provide further information concerning the environments experienced by Nile Red, the spectra of the ternary systems were decomposed into component spectra. Because of the asymmetric nature of the Nile Red spectrum, the measured spectra were fitted to the sum of log-normal functions, an approach previously used to model the asymmetric spectra of hydroxypyridine.[35] This methodology has previously been used to model Nile Red spectra in inclusion complexes in γ-cyclodextrin,[27] as well as when the dye is

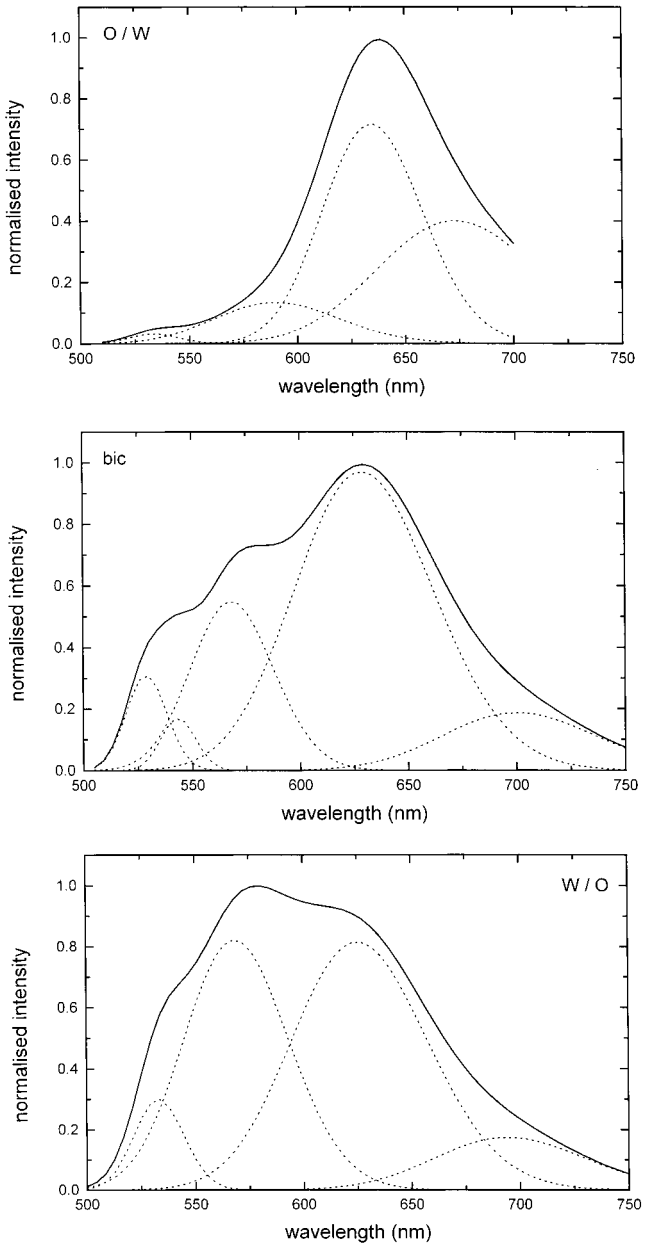

Figure 3. Fitted sum spectra and component spectra obtained for Nile Red in the ternary systems.

incorporated in sol−gel-derived media.[36] The results obtained, shown in Figure 3, confirm the analysis given above. In the water-rich region over 60% of the Nile Red emission can be assigned to the dye in $C_{12}E_5$ close to the headgroup experiencing the higher dielectric constant of the water. In the bicontinuous region nearly half of the emission can be associated with the dye in tetradecane, with a majority of the remainder arising from the probe interacting with $C_{12}E_5$. These results are similar to those obtained for the oil-rich region, except that in this case there is slightly more emission associated with Nile Red in tetradecane. Making use of the solvent scale shown in Figure 2, if we consider the main emission in the o/w region, then values of 48.5 and 51 for E_{NR} and $E_{T(30)}$ respectively are obtained. In the bicontinuous region 50.3, 45.5 and 34, 49 for E_{NR} and $E_{T(30)}$ are recovered for the main emissions. Finally, for the w/o region, the main emissions yield values of 50.3 and 45.7 for E_{NR} while 34 and 47 are recovered for $E_{T(30)}$.

Time-Resolved Data. Although the position of the emission spectrum of Nile Red is heavily influenced by the dielectric constant of its environment, there are reports that its time-resolved kinetics are more viscosity dependent.[34] With this in mind a time-resolved fluorescence study of the dye in the three ternary systems was performed. For ease of comparison an initial study was carried out on solutions of Nile Red in pure tetradecane and $C_{12}E_5$ at the different temperatures used for the ternary systems. The outcome is presented in Table 1. The fluorescence decay of Nile Red in tetradecane can be simply modeled as a single exponential whose decay time decreases with temperature. The fact that a good monoexponential decay could be obtained demonstrates the purity of the sample and the presence of a single emitting species. (Previous work[36] using the same batch of dye has also demonstrated single exponential decays in a variety of solvents.) Using $C_{12}E_5$ as the solvent, however, the kinetics of the decay are more complex. Here, to fit the decay a sum of three exponential components has to be used. At this stage, for the sake of simplicity, only one excitation and emission wavelength were used, although in viscous systems, such as $C_{12}E_5$ (using time-resolved anisotropy and Rhodamine 6G as a probe, we have obtained[37] values of viscosity of 19.2×10^{-3}, 15.6×10^{-3}, and 11.2×10^{-3} N m^{-2} s for $C_{12}E_5$ at 34, 45, and 57 °C, respectively), it is known that the formation of a solvent relaxed state can manifest itself by the presence of an initially excited state with a shorter lived decay, whose preexponential factor is emission wavelength dependent.[34] The recovered decay time τ_2 is similar in magnitude to that obtained in pure tetradecane, so it is likely to arise from the probe interacting with the nonpolar tail region of the surfactant. The longer lived component is similar to that observed in solvents of raised dielectric constants and thus can relate to the dye interacting with the head region of the surfactant. Also, it should be noted that the polarity of the surfactant headgroup has been found to vary according to its conformation,[38] a fact that should be borne in mind as the conformational freedom will differ between the pure solvent and the different ternary systems. At this point the shortest lived component is harder to ascribe and could relate to either the effects of solvent relaxation or a ground state inhomogeneity observed in some nonpolar solvents.[34] Because of the viscosity of the $C_{12}E_5$ the former is most probable.

The data recovered for Nile Red in the three regions, for different emission wavelengths, are presented in Table 2. In principle the decays monitored at 550 nm should relate more to emission from dye in tetradecane, that at 600 nm from dye in a tetradecane/surfactant environment, and that at 650 nm to more a water influenced surfactant environment. The table shows that a majority of the decays can be fitted using a sum of two exponential components. Also present in the data, as with that for pure $C_{12}E_5$, are "rise times" or negative preexponential factors, which exhibit a wavelength dependency. These have previously been observed using Nile Red in viscous media and have been associated with the formation of a solvent relaxed state,[34] which is not surprising considering the viscosity of these systems. For the oil-in-water system we have measured a viscosity of ca. 10×10^{-3} N m^{-2} s (from Rhodamine 6G anisotropy measurements[37]) with a value of 8.1×10^{-3} N m^{-2} s obtained for the bicontinuous region.[18] Using the same method we also obtained a value of 6.1×10^{-3} N m^{-2} s for the oil-rich region. Generally, the longer lived (τ_1) component appears to describe an environment between that of tetradecane and the headgroup of the surfactant. Also, considering the data set as a whole, there appear to be more similarities between the water-rich and bicontinuous regions than there are between these regions and the oil-rich region. This is not too surprising because

TABLE 1: Time-Resolved Decay Data for Nile Red in Pure Solvents

solvent	temp (°C)	λ_{exc}, λ_{em} (nm)	τ_1 (ns)	α_1	τ_2 (ns)	α_2	τ_3 (ns)	α_3	χ^2
tetradecane	34	500, 550	2.76 ± 0.02	1					1.10
	45		2.44 ± 0.02	1					1.20
	57		2.09 ± 0.01	1					1.14
$C_{12}E_5$	34	490, 600	4.27 ± 0.08	0.43	2.44 ± 0.45	0.27	0.39 ± 0.18	0.30	1.08
	45		4.30 ± 0.09	0.40	2.44 ± 0.45	0.27	0.43 ± 0.15	0.33	1.07
	57		4.19 ± 0.07	0.37	1.97 ± 0.30	0.33	0.46 ± 0.21	0.30	1.09

TABLE 2: Recovered Decay Parameters for Nile Red at Various Emission Wavelengths (λ_{em}) with an Excitation Wavelength (λ_{exc}) of 490 nm in the Ternary System of $C_{12}E_5$/Water/Tetradecane for the Different Region

	λ_{em}	τ_1 (ns)	α_1	τ_2 (ns)	α_2	τ_3 (ns)	α_3	χ^2
o/w	550	2.57 ± 0.06	0.11	0.99 ± 0.09	0.36	0.25 ± 0.18	0.53	1.23
	600	2.94 ± 0.02	0.57	0.83 ± 0.09	0.43			1.16
	650	3.01 ± 0.02	0.64	0.79 ± 0.08	−0.36			1.18
	700	3.01 ± 0.03	0.59	1.63 ± 1.08	−0.07	0.63 ± 0.15	−0.34	1.25
bic	550	3.20 ± 0.35	0.15	1.28 ± 0.12	0.17	0.10 ± 0.10	0.68	1.11
	600	3.16 ± 0.03	0.65	1.19 ± 0.15	0.35			1.08
	650	2.94 ± 0.03	0.64	0.55 ± 0.07	−0.36			1.26
	700	2.95 ± 0.03	0.62	0.54 ± 0.06	−0.38			1.20
w/o	550	3.37 ± 0.27	0.55	1.27 ± 0.12	0.45			1.17
	600	3.66 ± 0.03	0.74	1.98 ± 0.39	0.26			1.19
	650	3.51 ± 0.03	0.49	1.32 ± 0.39	0.15	0.56 ± 0.33	−0.36	1.19
	700	4.97 ± 0.42	0.07	3.09 ± 0.24	0.67	0.59 ± 0.18	−0.26	1.22

of the hydrophobic nature of the dye, which means that it can be found in the bulk solvent in the w/o region, but confined to oil and surfactant areas in the other regions.

To see if any further trends could be elucidated, the data from each of the regions were analyzed globally by linking the decay times. In each case a sum of four exponential decays were required to give an adequate fit. The results are displayed in Figure 4 and for ease of comparison other decay time components (those at 2.05 and 3.8 ns) have been included in the plots for each region (although not recovered in the analysis) and their values presented as zero. From these data, again, the existence of wavelength-dependent rise times can be observed. The magnitudes of the recovered decay times are, within error, similar and the quantity of the negative component increases with wavelength. Also common to each region is a decay component ranging from 0.91 to 1.26 ns. Its wavelength dependency appears similar throughout the ternary systems; i.e., the quantity is found to decrease with increasing wavelength, which could relate to tetradecane associated emission. The next component, in terms of decay time (2.05 ns), is only recovered for Nile Red in the water-rich region. In this region the dye is situated within oil-filled micelles with hydrodynamic radii of about 80 Å.[39] The steady state spectrum of Nile Red in this phase indicates that the major emission comes from dye situated close to the surfactant headgroup. Another decay component common to all the regions is one close to 3 ns, the wavelength dependency of which is different in each region. In the o/w region the larger quantity is obtained at the emission wavelength of 600 nm. In the bicontinuous region this occurs at 650 nm, and in the w/o region it occurs at 550 nm. Overall, it appears that this component is associated more with the alkane or surfactant tail, as is the longest lived decay component of 3.8 ns, which is more dominant in the w/o region.

Prodan. This probe was found to be soluble in each of the constituent solvents and hence should partition throughout the ternary systems. It exhibits large spectral shifts depending on the dielectric constant of its environment, along with changes in lifetime and quantum yield.[40]

Steady State Data. The peak fluorescence emission of Prodan in the constituent pure solvents exhibits a shift of over 120 nm between Prodan emission in tetradecane (397 nm) and in water (520 nm). The peak emission in $C_{12}E_5$ is located between these at 461 nm; see Figure 5. The equal spacing of the peak emissions and the fact that Prodan is soluble in each of the constituent chemicals show that this probe could prove useful in obtaining a global picture of these systems. The relative fluorescence yields of Prodan in the pure tetradecane and $C_{12}E_5$ were found to be similar, although in water it was approximately 6 times higher.

The spectra obtained for Prodan in each of the different regions are also depicted in Figure 5. This shows peak emission at 493 nm for Prodan in the o/w region, 492 nm in the bic region, and 417 nm for the w/o region. This indicates that in the water-rich and bicontinuous regions the major emission comes from Prodan located in an environment with a greater polarity than $C_{12}E_5$, but less than water. Hence, the most likely position is that the probe is in the surfactant headgroup, affected by the influence of the aqueous environment. The inset in Figure 5 bears this out and shows that the major emission of this probe comes from Prodan located in this position. It should be noted that studies have shown that water confined within nanocavities can exhibit a significantly lower dielectric constant than bulk water,[41] so emission from probe located within small water pools cannot be completely ruled out. As with Nile Red, the biggest effect was observed in the oil-rich region. This can be seen in the inset, which shows that the peak emission wavelength changes from close to 410 nm (emission from a low-polarity environment) for shorter excitation wavelengths to the longer wavelength emission seen in the other two regions for longer excitation wavelengths. This can be explained by the partitioning of the probe between two main environments, i.e., the oil/oil−surfactant tail and the surfactant headgroup.

Again to quantify the polarity of the environment in which Prodan is partitioned, the peak emission wavelength of this probe was recorded in a variety of different solvents and the outcome in relation to both dielectric constant and $E_{T(30)}$ is presented in Figure 6. The relation between dielectric constant and peak emission wavelength is clearly not a linear one. The values of the peak fluorescence are found to be higher when using protic solvents in comparison to nonprotic ones. This can relate to the hydrogen bonding properties of Prodan.[40] In relation to this fact, however, a good linear relationship is obtained between the peak emission and the $E_{T(30)}$ scale. A linear relationship between peak emission and dielectric constant can be obtained

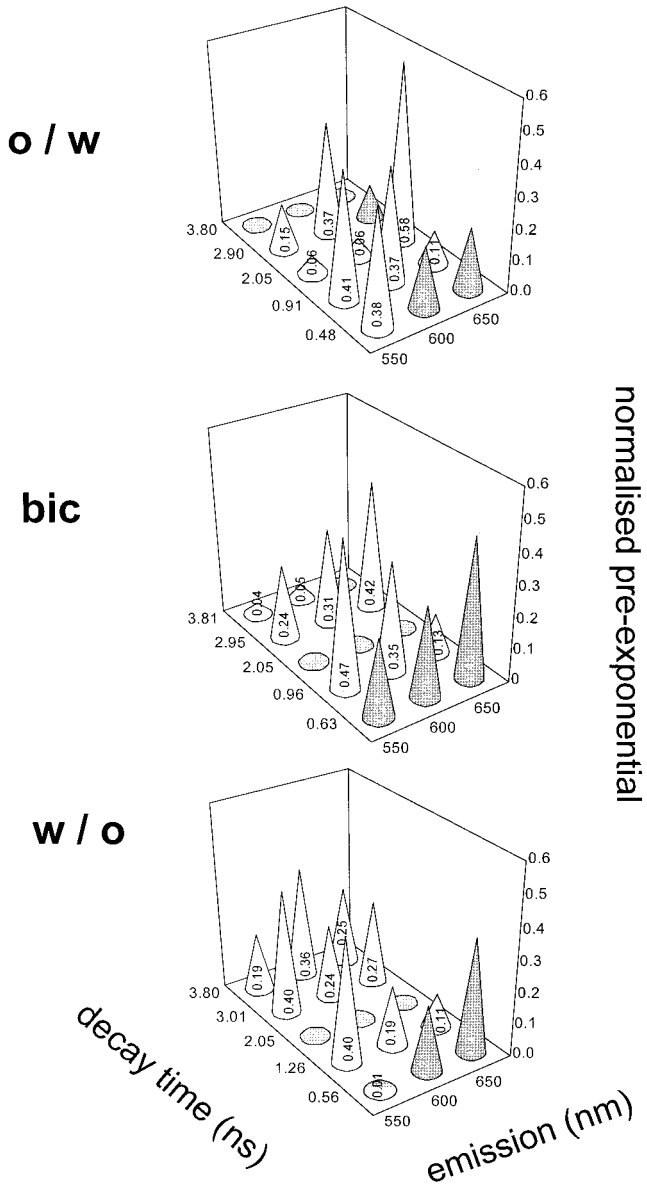

Figure 4. Representation of the outcome of the global analysis of the time-resolved data for different emission wavelengths of Nile Red in the ternary systems. The shaded components indicate a rise time.

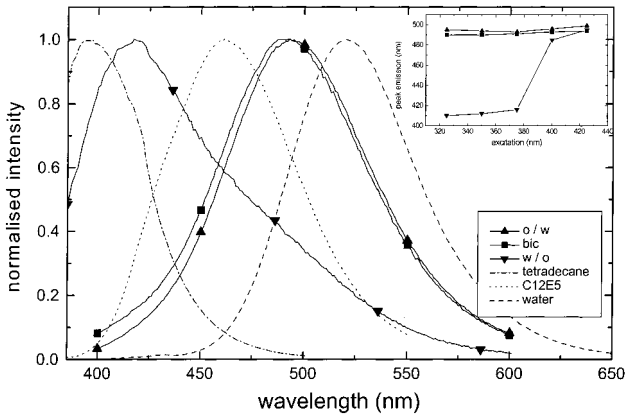

Figure 5. Steady state fluorescence of Prodan, excited at 375 nm, in the ternary system and in component pure solvents. The effect of changing the excitation wavelength on the peak fluorescence emission is shown in the inset.

if just protic solvents are considered, as has been demonstrated for Prodan in buffered binary solutions.[42] In our case it could be possible to make use of this fact, but considering the range of environments encountered and to make a comparison with the Nile Red data, it seems more appropriate to use the $E_{T(30)}$ scale once more. The positions of the peak emission in the three regions yield $E_{T(30)}$ values of 54.1, 53.9, and 35.0 for the o/w, bic, and w/o regions, respectively. Again, as these spectra result from the sum of the spectra of Prodan partitioned into different environments, gaining a fuller picture reconvolution of these spectra is required. However, a quick comparison of these values with those obtained for Nile Red show that overall Prodan favors a slightly more polar environment, but with both probes located in a similar environment in the oil-rich region.

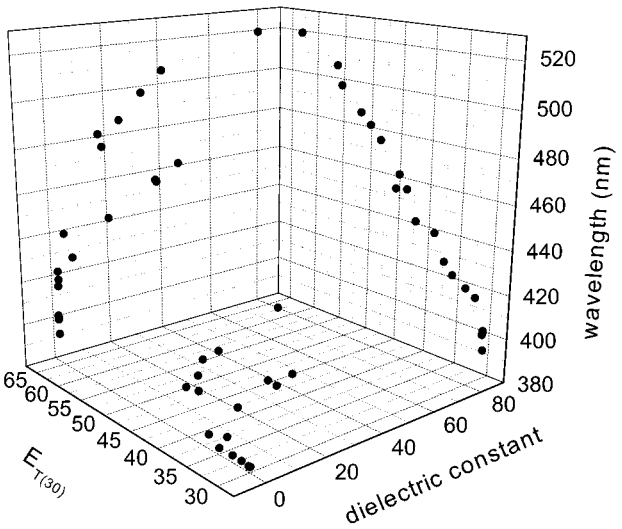

Figure 6. Position of the Prodan peak emission for various solvents related to both dielectric constant and the $E_{T(30)}$ scale.

Decomposition of Fluorescence Spectra. Again, to obtain further information, the emission spectra were decomposed into component spectra to ascertain how the Prodan is partitioned. These spectra are displayed in Figure 7. As in the case of Nile Red, most similarities are observed between the water-rich and bicontinuous regions. The main components in these regions emit close to 485 and 520 nm. These relate to emission from dye in the proximity of the $C_{12}E_5$ head and in water, respectively. As the fluorescence yield in water is ca. 6 times that in the other pure constituent solvents, a great proportion of this probe should be partitioned in the surfactant. In the o/w region it is unsurprising to find Prodan in free water, but in the bic region the results indicate that a reasonable amount is located in the water channels. Thus the combination of the use of the two probes Nile Red and Prodan appear complementary in reporting on the interfaces on either side of the water−surfactant−oil boundary.

The component spectra obtained for Prodan in the oil-rich region show that the major emission of the probe pertains to an environment with a low dielectric constant, most likely in the tetradecane with some interaction with the surfactant tail. Also, emissions relating to probe situated in water and surfactant headgroup are present.

To quantify the polarity of the Prodan environment, we can consider the two major emissions (these contribute over 80% of the fluorescence in each spectrum) present in each region in terms of the $E_{T(30)}$ scale. In the water-rich regions the emissions at 486 and 524 nm relate to values of 52.4 and 62.0. In the bicontinuous region the emissions at 482 and 520 nm return values of 51.4 and 61.0. Finally, in the w/o region the emissions at 413 and 462 nm correspond to values of 34.0 and 46.3, respectively. This shows that a majority of the Prodan fluores-

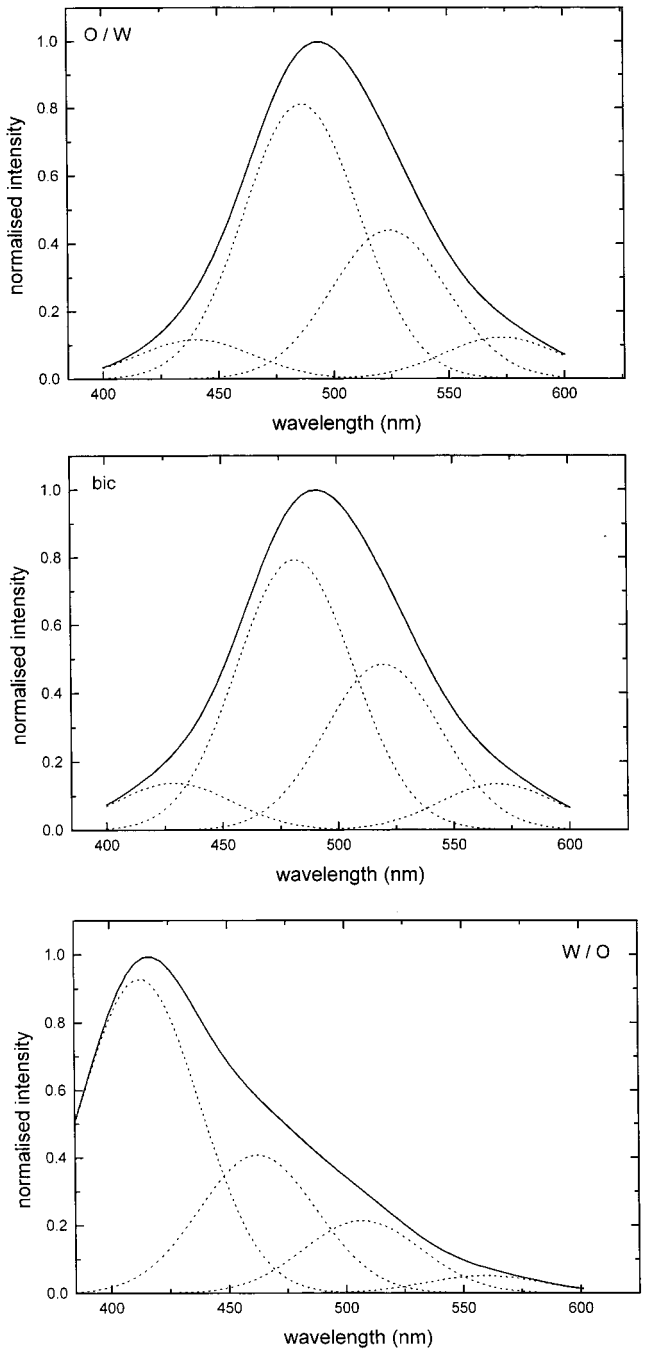

Figure 7. Fitted sum spectra and component spectra obtained for Prodan in the ternary systems.

cence in the o/w and bic regions relates to the probe situated in similar environments. In the w/o region Prodan is partitioned into a less polar environment, similar to that encountered by the Nile Red.

Time-Resolved Data. As with Nile Red the initial step involved monitoring the fluorescence decay of Prodan in the constituent pure solvents. This was carried out at each of the temperatures used to support the three regions. The results obtained are given in Table 3. In pure surfactant the decay can be adequately described using a single exponential model. In tetradecane two decay times were required to produce a good fit, although over 99% of the decay was related to the short (around 150 ps) component. For clarity only this decay time is presented (longer lived omitted). With both these solvents a decrease in decay time was observed with increasing temperature. Using water as the solvent, the decay kinetics become more complex and the sum of either two or three exponentials is required to model the decay. This is in keeping with the two exponential decay found by Balter et al.,[40] although exact comparison is not possible because of the different experimental conditions used. In all cases, however, the major components recovered have subnanosecond decay times and a small proportion of a component those decay time decreases from 1.67 to 1.37 ns on increasing temperature. Previous work using Prodan in butanol has detected wavelength-dependent fluorescence decays, which have been related to locally excited and charge transfer states.[43] An investigation in a range of protic and nonprotic solvents has also found multiexponential decays for Prodan.[40] In the case of protic solvents the possibility of hydrogen bond formation between probe and solvent was proposed. Certainly the excited kinetics of this probe in pure solvents are not simple, but the data that we have recovered should allow for some interpretation of the results obtained in the ternary systems.

The data recovered for Prodan in the $C_{12}E_5$/water/tetradecane systems are presented in Table 4, where an excitation wavelength of 375 nm was used and the emission was monitored at different specific wavelengths or wavelength ranges. Because of this, the results obtained for each region were analyzed globally by linking the decay times. As in the case of Nile Red, wavelength-dependent subnanosecond rise times are recovered, which it is tempting to ascribe in a similar manner. Greater amounts of these components are observed at longer emission wavelengths. As well as the influence of the oil and surfactant viscosity, also water when constrained within surfactant systems has been found to exhibit slower dielectric relaxation[44] and can influence the probe's solvation dynamics. The other decay times recovered are slightly longer than that found for the longer lived component of Prodan in water, but shorter than that obtained for the probe in pure $C_{12}E_5$. It should be noted that because of the wavelengths used little, if any, emission from Prodan in a purely tetradecane-like environment should be observed. The wavelength ranges were determined by the LED excitation source and the use of filters to avoid scattered excitation light. Emission at 500 nm should to a major degree relate to Prodan in the surfactant head−water interface, while that at 550 nm relates to the probe in water. The range >435 nm should also include the probe in the oil−surfactant interface.

The relative amounts of the two longer lived decays also exhibit a wavelength dependency (as shown by the α_1/α_2 ratio) with an apparent increase in the amount of the longest lived component at 550 nm, possibly linking this to emission in a more aqueous environment. Comparing the ratios of the preexponential factors of these decay times across the ternary systems, greater similarities are recovered between the bicontinuous and oil-rich regions in comparison to the water-rich region, although caution should be exercised as emission from Prodan in a low-polarity environment is not fully accounted for.

4-Di-1-ASP. Finally, to complement the other two probes, the water-soluble dye 4-Di-1-ASP was chosen, as it has low solubility in tetradecane and has been shown to exhibit solvent dependent fluorescence behavior.[31] Thus, it appeared an interesting probe to use in conjunction with Nile Red and Prodan.

The fluorescence spectra for this dye in pure solvents (surfactant and water) plus the ternary systems are shown in Figure 8. Although 4-Di-1-Asp displays a different peak emission when in pure $C_{12}E_5$ (587 nm) and water (606 nm), when incorporated into the ternary systems not much difference can be observed between the three regions. Changing the

TABLE 3: Time-Resolved Data for Prodan in Pure Solvents with an Excitation Wavelength of 375 nm

solvent	temp (°C)	λ_{em} (nm)	τ_1 (ns)	α_1	τ_2 (ns)	α_2	τ_3 (ns)	α_3	χ^2
tetradecane	34	>420	0.20 ± 0.01	0.995					1.01
	45		0.16 ± 0.01	0.998					1.15
	57		0.12 ± 0.01	0.998					1.00
water	34	>435	1.67 ± 0.03	0.22	0.49 ± 0.03	0.78			1.08
	45		1.49 ± 0.04	0.08	0.64 ± 0.12	0.17	0.12 ± 0.12	0.75	1.14
	57		1.37 ± 0.05	0.06	0.62 ± 0.11	0.20	0.13 ± 0.12	0.74	1.17
$C_{12}E_5$	34	>420	3.68 ± 0.01	1					1.05
	45		3.64 ± 0.01	1					1.08
	57		3.62 ± 0.02	1					1.09

TABLE 4: Global Analysis for the Decay of Prodan in the Ternary System for the Different Regions Giving the Preexponential Factors for the Recovered Lifetime Values[a]

o/w, Global $\chi^2 = 1.12$

	decay component (ns)				
λ_{em}	0.47 ± 0.10	2.51 ± 0.43	3.39 ± 0.18	χ^2	α_2/α_3
>435	−0.22	0.57	0.21	0.98	2.7
>495	−0.43	0.41	0.16	1.20	2.6
500	−0.38	0.49	0.13	1.21	3.8
550	−0.51	0.36	0.13	1.07	2.7

bic, Global $\chi^2 = 1.06$

	decay component (ns)				
λ_{em}	0.41 ± 0.11	1.88 ± 0.47	2.82 ± 0.06	χ^2	α_2/α_3
>435	−0.38	0.30	0.32	1.01	0.9
>495	−0.52	0.21	0.27	1.14	0.8
500	−0.43	0.27	0.30	1.05	0.9
550	−0.54	0.18	0.28	1.04	0.6

w/o, Global $\chi^2 = 1.18$

	decay component (ns)				
λ_{em}	0.36 ± 0.11	1.70 ± 0.38	2.77 ± 0.05	χ^2	α_2/α_3
>435	−0.46	0.28	0.26	1.19	1.1
>495	−0.58	0.19	0.23	1.09	0.8
500	−0.46	0.26	0.28	1.17	0.9
550	−0.59	0.17	0.24	1.27	0.7

[a] The excitation was at 375 nm. The ratios α_2/α_3 of the preexponential factors for the decay times are also shown.

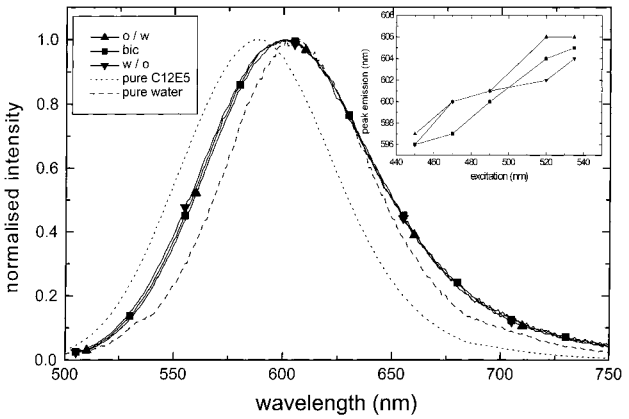

Figure 8. Steady state fluorescence of 4-Di-1-ASP, excited at 490 nm, in the ternary system and in component pure solvents. The effect of changing the excitation wavelength on the peak fluorescence emission is shown in the inset.

excitation wavelength (inset, Figure 8) produced an increase in the peak emission wavelength (of up to 10 nm) in each case. This can relate to a distribution of sites for the dye, i.e., between the water and interacting with the surfactant head. The spectra of the dye in the ternary systems also have a larger full width at half-maximum (fwhm) than in the constituent solvents. These data are provided in Table 5 and also hint at interaction with the surfactant. The decay times recovered are also presented in Table 5. Previous reports have obtained decay times of the order

TABLE 5: Steady State and Time-Resolved Data Showing Major (>99%) Decay Component for 4-Di-1-ASP in Pure Solvents and in the Different Regions of the Ternary System[a]

system	spectral fwhm (cm^{-1})	τ (ns)
$C_{12}E_5$	2409	0.56 ± 0.08
water	2126	
o/w	2504	0.20 ± 0.03
bic	2536	0.13 ± 0.02
w/o	2569	0.11 ± 0.02

[a] The time-resolved measurement in $C_{12}E_5$ was performed at 34 °C with 490 nm excitation and $\lambda_{em} = 600$ nm, with λ_{em} for the others >550 nm. The decay time in water was beyond the resolution of our equipment.

of 50 ps for this dye in ethanol.[31] In water the decay time was faster than our equipment could measure, while in pure surfactant a decay with a major decay time of 560 ps was recovered. The decays from the ternary systems are also fast and can relate to 4-Di-1-ASP at the surfactant head−water interface. Thus it appears that, because of the preference for an aqueous environment, with our equipment no data of the same quality obtained with Nile Red and Prodan could be recovered with this particular dye. Future work is planned to extend this study using higher time resolution.

Conclusion

We have demonstrated the complementary use of different fluorescent probes to report globally and from either side of

the water−surfactant−oil interface. The solvatochromic probes, Nile Red and Prodan, uncovered similarities between the water-rich and bicontinuous regions as evident from shifts in the peak fluorescence emission. In addition, they reveal that in the excited state lifetime different environments were encountered, which varied between water-rich and oil-rich domains. The time-resolved data, because of the viscosity dependence of some of the decay kinetics, proved useful in elucidating common features between the bicontinuous and oil-rich regions. Thus, these studies unveil the dual facets of the bicontinuous region.

Acknowledgment. Financial support from the Fundação para a Ciência e a Tecnologia, through the PRAXIS XXI program and Sapiens (POCTI/35415/QUI/2000), is acknowledged.

References and Notes

(1) Olsson, U.; Shinoda, K.; Lindman, B. *J. Phys. Chem.* **1986**, *90*, 4083.
(2) Lichterfeld, F.; Schmeling, T.; Strey, R. *J. Phys. Chem.* **1986**, *90*, 5762.
(3) Kahlweit, M.; Strey, R.; Hasse, D.; Kunida, H.; Schmeling, T.; Faulhaber, B.; Borkovec, M.; Eixke, H.-E.; Busse, G.; Eggers, F.; Funk, Th.; Rickman, H.; Magid, L.; Siderman, O.; Stilbs, P.; Winkler, J.; Dittrich, A.; Jahn, W. *J. Colloid Interface Sci.* **1987**, *118*, 436.
(4) Shinoda, K.; Kunieda, H.; Arai, T.; Saijo, H. *J. Phys. Chem.* **1984**, *88*, 5126.
(5) Kunieda, H.; Shinoda, K. *J. Dispersion Sci. Technol.* **1982**, *3*, 233.
(6) Kahlweit, M.; Strey, R. *Angew. Chem., Int. Ed. Engl.* **1985**, *24*, 654.
(7) Aveyard, R.; B. P. Binks, B. P.; Fletcher, P. D. I. *Langmuir* **1989**, *5*, 1210.
(8) Olsson, U.; Wurz, U.; Strey, R. *J. Phys. Chem.* **1993**, *97*, 4535.
(9) Leaver, M. S.; Olsson, U.; Wennerstrom, H.; Strey, R.; Wurz, U. *J. Chem. Soc., Faraday Trans.* **1995**, *91*, 4269.
(10) Scriven, L. E. *Nature* **1976**, *263*, 123.
(11) Lindman, B.; Kamenka, N.; Kathopoulis, T.-M.; Brun, B.; Nillson, P.-G. *J. Phys. Chem.* **1980**, *84*, 2485.
(12) Olsson, U.; Wennerstrom, H. *Adv. Colloid Interface Sci.* **1994**, *49*, 113.
(13) Real Oliveira, M. E. C. D.; Hungerford, G.; Castanheira, E. M. S.; Miguel, M. da G.; Burrows, H. D. *J. Fluoresc.* **2000**, *10*, 347.
(14) Slavik, J. *J. Fluoresc.* **1997**, *7*, 49s.
(15) Karukstis, K. K.; Suljak, S. W.; Waller, P. J.; Whiles, J. A.; Thompson, E. H. Z. *J. Phys. Chem.* **1996**, *100*, 11125.
(16) Karukstis, K. K.; Frazier, A. A.; Loftus, C. T.; Tuan, A. S. *J. Phys. Chem. B* **1998**, *102*, 8163.
(17) Sengupta, B.; Guharay, J.; Sengupta, P. K. *Spectrochim. Acta, Part A* **2000**, *56*, 1433.
(18) Real Oliveira, M. E. C. D.; Hungerford, G.; Miguel, M. da G.; Burrows, H. D. *J. Mol. Struct.* **2001**, *563−564*, 443.
(19) Weber, G.; Farris, F. J. *Biochemistry* **1979**, *18*, 3075.
(20) Greenspan, P.; Fowler, S. D. *J. Lipid Res.* **1985**, *26*, 781.
(21) Mazumdar, M.; Parrack, P. K.; Bhattacharyya, B. *Eur. J. Biochem.* **1992**, *204*, 127.
(22) Bunker, C. E.; Bowen, T. L.; Sun, Ya-Ping. *Photochem. Photobiol.* **1993**, *58*, 499.
(23) Sackett, D. L.; Wolff, J. *Anal. Biochem.* **1987**, *167*, 228.
(24) Davis, D. M.; Birch, D. J. S. *J. Fluoresc.* **1996**, *6*, 23.
(25) Maiti, N. C.; Krishna, M. M. G.; Britto, P. J.; Periasamy, N. *J. Phys. Chem. B* **1997**, *101*, 11051.
(26) Datta, A.; Mandal, D.; Pal, S. K.; Bhattacharyya, K. *J. Phys. Chem. B* **1997**, *101*, 10221.
(27) Srivatsavoy, V. J. P. *J. Lumin.* **1999**, *82*, 17.
(28) Dutt, G. B.; Doriswamy, S.; Periasamy, N. *J. Phys. Chem.* **1991**, *94*, 5360.
(29) Dutt, G. B.; Doriswamy, S. *J. Phys. Chem.* **1992**, *96*, 2475.
(30) Deye, J. F.; Berger, T. A.; Anderson, A. G. *Anal. Chem.* **1990**, *62*, 615.
(31) Strehmel, B.; Rettig, W. *J. Biomed. Opt.* **1996**, *1*, 98.
(32) Huebner, J. S.; Varnadore, W. E., Jr. *Photochem. Photobiol.* **1982**, *35*, 141.
(33) Birch, D. J. S.; Hungerford, G. In *Topics in fluorescence spectroscopy*; Lakowicz, J. R., Ed.; Plenum Press: New York, 1994; Vol. 4, p 377.
(34) Krishna, M. M. G. *J. Phys. Chem. A* **1999**, *103*, 3589.
(35) Siano, D. B.; Mettzler, D. E. *J. Chem. Phys.* **1969**, *51*, 1856.
(36) Hungerford, G.; Ferreira, J. A. *J. Lumin.* **2001**, *93*, 155.
(37) Hungerford, G.; Real Oliveira, M. E. C. D.; Castanheira, E. M. S.; Burrows, H. D.; Miguel, M. da G. Submitted for publication in *Prog. Colloid. Polym. Sci.*
(38) Medhage, B.; Almgren, M.; Alsins, J. *J. Phys. Chem.* **1993**, *97*, 7753.
(39) Bagger-Jörgensen, H. Polymer effects on microemulsions and lamellar phases. Ph.D. Thesis, Lund University, Sweden, 1997, and references therein.
(40) Balter, A.; Nowwak, W.; Pawełkiewicz, W.; Kowalczyk, A. *Chem. Phys. Lett.* **1988**, *143*, 565.
(41) Senapati, S.; Chandra, A. *J. Phys. Chem. B* **2001**, *105*, 5106.
(42) Harianawala, A. I.; Bogner, R. H. *J. Lumin.* **1998**, *79*, 97.
(43) Heisel, F.; Miehé, J. A.; Szemik, A. W. *Chem. Phys. Lett.* **1987**, *138*, 321.
(44) Bhattacharyya, K.; Bagchi, B. *J. Phys. Chem. A* **2000**, *104*, 10603.